Electronic Supporting Information

Artificial heme-enzyme with enhanced catalytic activity: evolution, functional screening and structural characterization.

Rosa Vitale,[a] Liliana Lista,[a] Corinne Cerrone,[a] Giorgio Caserta,[b] Marco Chino,[a] Ornella Maglio,[a,c] Flavia Nastri,[a] Vincenzo Pavone,[*,a,d] Angela Lombardi[*,a,d]

[a] Department of Chemical Sciences, Complesso Universitario Monte S. Angelo, University of Naples "Federico II". Via Cintia, 80126 Naples, Italy. E-mail: vincenzo.pavone@unina.it, angela.lombardi@unina.it

[b] Collège de France, 11 place Marcelin Berthelot, 75231 Paris Cedex 05, France

[c] IBB, CNR, Via Mezzocannone 16, 80134 Naples , Italy

[d] IMAST Scarl Piazza Bovio 22, 80133 Naples, Italy,

Materials and instrumentation

All Fmoc (9-fluorenylmethoxycarbonyl) protected amino acids, NovaSyn TG Sieber resin, and coupling reagents (HOBt, 1-Hydroxybenzotriazole, HATU, 1-[Bis(dimethylamino)methylene]-1H-1,2,3-triazolo[4,5-b]pyridinium 3-oxid hexafluorophosphate, and PyBOP, (Benzotriazol-1-yloxy)tripyrrolidinophosphonium hexafluorophosphate) were purchased from Novabiochem. All solvents, used in the synthesis and purification, were anhydrous and HPLC grade, respectively, and were supplied by Romil. Piperidine and scavengers (ethanedithiol, triisopropylsilane) were from Fluka. TFA (trifluoroacetic acid) and DIPEA (N, N-Diisopropylethylamine) were from Applied Biosystems. Pre-coated silica G-60 plates, F254, used for thin-layer chromatography (TLC), were from Merck. Deuteroporphyrin IX was from Porphyrin Products. Iron (II) acetate was purchased from Sigma Aldrich. All buffer solutions were made by using water with a HPLC purity grade (Romil); phosphate salts (monobasic and dibasic) for buffers preparation, were provided by Fluka; TFE (2,2,2-Trifluoroethanol) was supplied from Romil. The substrates ABTS and H_2O_2 (30%, v/v), used in the catalytic assays, were purchased from Sigma and Fluka, respectively.

Protected peptides were obtained by the use of ABI 433 automatic peptide synthesizer (Applied Biosystems, Foster City, CA, USA). HPLC and LC-MS analysis were performed with a Shimadzu LC-10ADvp equipped with an SPDM10Avp diode-array detector. ESI-MS spectra were recorded on a Shimadzu LC-MS-2010EV system with ESI interface, Q-array-octapole-quadrupole mass analyzer, and Shimadzu LC-MS solution Workstation software for data processing. The optimized MS parameters were selected as followed: CDL (curved desolvation line) temperature 250 °C; the block temperature 250 °C; the probe temperature 250 °C; detector gain 1.6kV; probe voltage +4.5kV; CDL voltage -15V. Nitrogen served as nebulizer gas (flow rate: 1.5 L/min). Flash Chromatography was performed using a Biotage Isolera flash purification system, equipped with a diode-array detector. UV-vis analysis was performed on Cary Varian 50 Probe UV Spectrophotometer; CD analysis was carried out on Jasco J-815 dichrograph, equipped with a 45MM electromagnet (model 340).

All the data were analyzed by using the Origin Pro 8 and the Kaleidagraph software.

Synthesis procedure

MC6 analogues were synthesized combining solution and solid-phase peptide methods, as described for MC-6 and MP3.[1,2] The two peptides were obtained by automated solid-phase synthesis, using the Fmoc protection strategy. A Sieber resin (0.2mmol/g loading) was chosen for the synthesis, on a 0.25-mmol scale, because it allows the cleavage of the fully protected peptide chains under very mild conditions[3]. For the synthesis of the peptides the following amino acids were used:

- ✓ Fmoc-Asp (OtBu)-OH; Fmoc-Glu(OtBu)-OH; Fmoc-Gln(Trt)-OH; Fmoc-Leu-OH; Fmoc-Ser(tBu)-OH; Fmoc-Lys(Mmt)-OH; Fmoc-Arg (Pbf)-OH: for MC-6 decapeptide chains.
- ✓ Fmoc-Asp(OtBu)-OH; Fmoc-Gln(Trt)-OH; Fmoc-Leu-OH; Fmoc-His(Trt)-OH; Fmoc-Ser(tBu)-OH; Fmoc-Lys(Mmt)-OH; Fmoc-Arg(Pbf)-OH; Fmoc-Lys(Boc)-OH; Fmoc-Ile-OH; Fmoc-Thr(tBu)-OH: for MC-6 tetradecapeptide chains.

Once eliminated the Fmoc group from the resin, cyclic deprotection, coupling and capping steps were repeated with each amino acid, until the chain assembly was completed.[2]

Peptides N-terminal amino groups were finally acetylated with Ac_2O/HOBt/DIEA solution in NMP. The subsequent synthetic procedures are summarized in Figure S1, where the two peptides are called (*TD*) and (*D*) to identify the 14-residue and 10-residue chains, respectively (please, refer to the Fig. 1 in the main text for amino acid numbering).

After the final step of the solid-phase synthesis, the N-ε Mmt protecting group of the Lys^9 residues, in both (*TD*) and (*D*) chains, were removed by repeated treatments (15 min, under gentle agitation) with a solution containing 10% acetic acid and 20% TFE (v/v) in CH_2Cl_2. Subsequently, in order to release the fully protected peptide from the resin, 3-4 resin volumes of a freshly prepared cleavage mixture (1% TFA in DCM, v/v) were added. The acidic mixture was incubated for 2 minutes, under mixing, and the solution was filtered with a vacuum pump, into an ice-cold flask containing 2 mL of 10% pyridine/methanol (v/v).

The peptides elution was controlled by TLC analysis, by using as eluent a chloroform/methanol mixture (90/10 v/v); each step was repeated until no product was detected in the collected fractions. The fractions containing the product were pooled and then evaporated under reduced pressure up to 5% of the volume. Ice-cold water was added and the mixture was cooled on ice to aid precipitation of the protected peptide. The product was washed several times, with fresh cold water and centrifuged at each step (4 min at 4°C, at 3300 g). Finally, it was dried under vacuum to give the crude peptides, which resulted amidated at the C-termini. Orthogonal side chain protecting groups were found to be stable in both Mmt deprotection and cleavage reactions.

Peptide identity was checked via LC-MS analysis, using a Vydac C8 column (4.6 mm·150 mm; 5 μm). The mobile phase was made up of H_2O/0.1% trifluoroacetic acid (TFA) (solvent A) and CH_3CN/0.1% TFA (solvent B); a linear gradient, from 50% to 90% of solvent B, over 40 min, at a 0.5 mL/min flow rate, was used.

After Mmt deprotection and cleavage from the resin, peptides were coupled in solution with the deuteroporphyrin IX (DP IX), by following the scheme in figure S1. MC6 (*D*) chain was first coupled to a large excess of DPIX to obtain the protected (*D*)-DPIX mono-adduct. This (*D*)-DPIX adduct was divided in two aliquots that were alternatively coupled to E^2L(*TD*) and $R^{10}L$(*TD*) chains, to obtain the corresponding analogs. The same approach was used to construct decapeptide analogs, with the E^2L and $R^{10}L$ substitutions, respectively. In this case the starting point was the (*TD*)-DPIX mono-adduct.

The first peptide-deuteroporphyrin conjugation was conducted in the presence of DIEA (7 equivalents), HATU (1 equivalent), and DPIX (1.5 equivalents). In order to avoid the formation of homodimers, this reaction was conducted in diluted solution ($7.2 \cdot 10^{-5}$ M peptide concentration in DMF) and by adding drop wise the first peptide to the deuteroporphyrin (30 adds every 2 minutes). The reaction mixture was stirred for

2 h at room temperature, and the pH was verified every 20 min, and adjusted with DIEA (pH ≈ 8.0), when necessary. The reaction was monitored both by analytical HPLC (Vydac C8 column; gradient: CH_3CN/H_2O, 0.1% TFA, 50% to 90% over 20 min, at 1 mL/min), and TLC (eluent: chloroform/methanol 90:10, v/v). Flash Chromatography was used between the two coupling steps, in order to eliminate the unreacted deuteroporphyrin. The crude products were purified on a SNAP HP 100 g silica column (5·30 cm), using a chloroform/methanol elution gradient from 0 to 15% methanol.

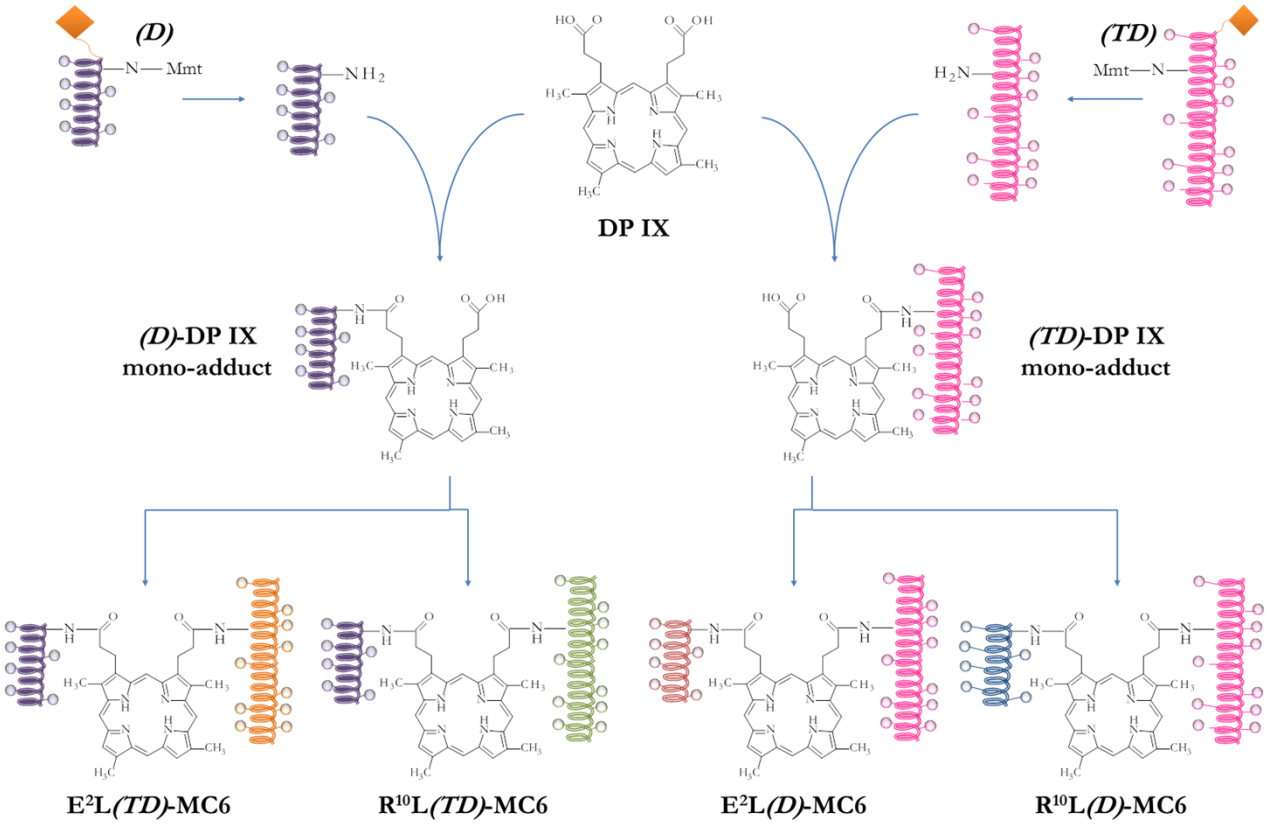

Figure S1: Synthetic strategy for MC-6 analogs. The chains are depicted in diverse colors to highlight the peptides combinations in the different analogues. The solid support used for the SPPS is depicted as an orange diamond, while the orthogonal protecting groups are shown as spheres.

Hence, the orthogonal protecting groups were removed by addition of the cleavage mixture (94% TFA, 2.5% EDT, 1% TIS, 2.5% H_2O, v/v). The reaction was conducted under stirring, at 0 °C for 1h, and at room temperature for a second hour. After concentration on a rotary evaporator, the scavengers were extracted and the crude product precipitated, by adding cold diethyl ether. The mixture was centrifuged (room temperature at 3300 g), the supernatant was removed and the precipitate was washed twice with three volumes of cold diethyl ether. The mixture was dried to remove diethyl ether, re-dissolved in water 0.1% TFA and analyzed by LC-MS, using a Vydac C18 column (4.6 mm·150 mm; 5 µm) with a gradient of acetonitrile in 0.1% aqueous TFA, 5% to 80% over 70 min, at 0.5 mL/min flow rate. The crude material was then purified by preparative RP-HPLC (Vydac 2.2 cm C18 column at 22 mL/min, using a gradient of CH_3CN in 0.1% aqueous TFA, 10% to 80% over 58.4 min).

The pooled fractions containing the desired product were lyophilized. Subsequently, iron ion was inserted, according to the acetate method procedure, slightly modified by us.[4,5] Iron (II) acetate (10 eq) was added to a solution of pure MC6 analogs free bases, in 2/3 TFE/AcOH (v/v) (c_{MC6}=2.0·10^{-4} M), and the reaction mixture

was kept at 50 °C for 2 h, refluxing under nitrogen. The reaction was monitored by analytical HPLC, using a Vydac C18 column, with an elution gradient of acetonitrile in 0.1% aqueous TFA, 5% to 80% over 35 min, at 1 mL/min flow rate. Once the reaction was completed, the solvent was removed under vacuum, and the product was purified to homogeneity by preparative RP-HPLC, following the procedure described above. After lyophilization, pure products were obtained as the TFA salt (yield 48%). LCMS analysis of all the analyzed compounds, which were obtained with high purity (>95%), confirmed the expected molecular weight (Fig. S2-S5). The analytical parameters of the obtained products are summarized in Table S1.

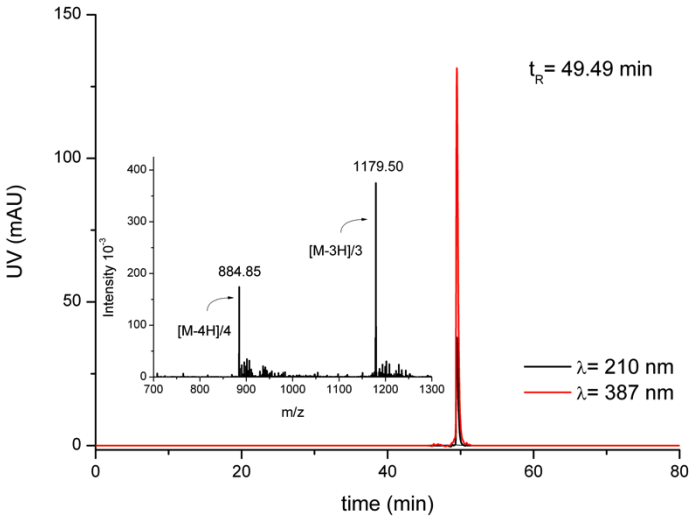

Figure S2: LC-MS chromatogram of pure Fe^{III}-E^{2}L(*TD*)-MC-6, and its positive ESI-MS m/z spectrum (inset). The peaks corresponding to the intact compound, carrying the indicated number of charges (protons), are evidenced.

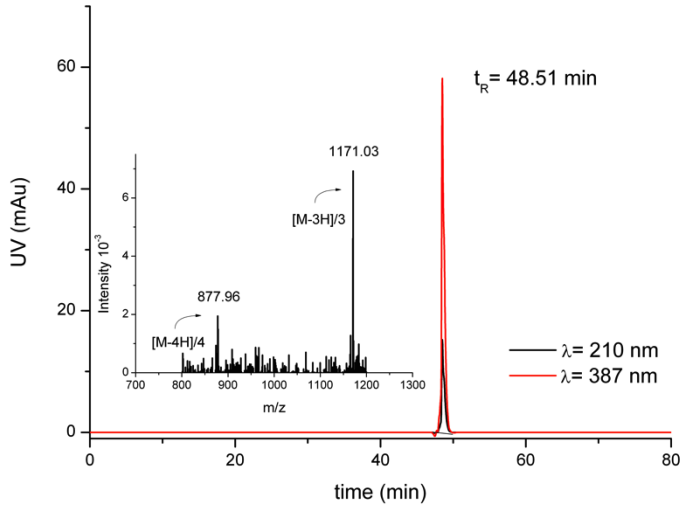

Figure S3: LC-MS chromatogram of pure Fe^{III}-R^{10}L(*TD*)-MC-6, and its positive ESI-MS m/z spectrum (inset). The peaks corresponding to the intact compound, carrying the indicated number of charges (protons), are evidenced.

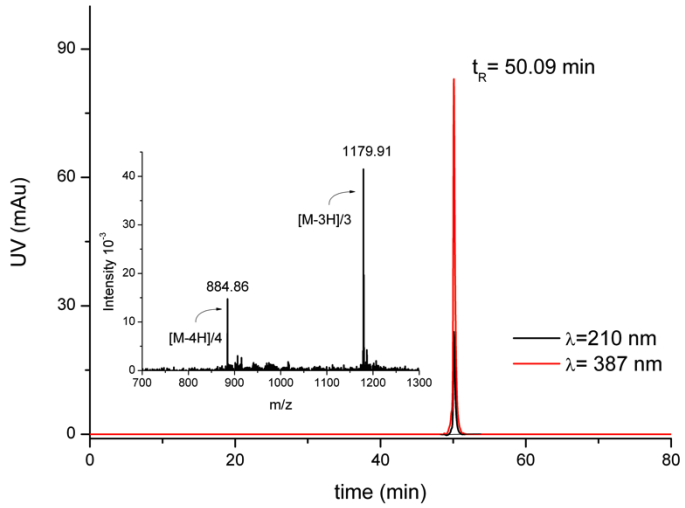

Figure S4: LC-MS chromatogram of pure Fe^{III}-$E^2L(D)$-MC-6, and its positive ESI-MS m/z spectrum (inset). The peaks corresponding to the intact compound, carrying the indicated number of charges (protons), are evidenced.

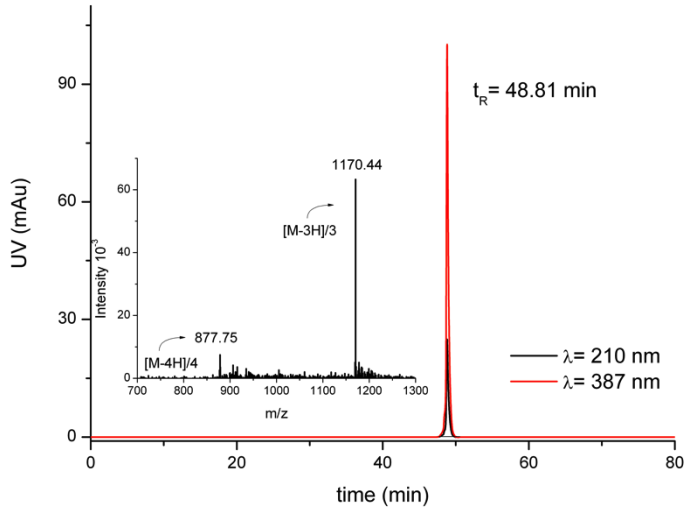

Figure S5: LC-MS chromatogram of pure Fe^{III}-$R^{10}L(D)$-MC-6, and its positive ESI-MS m/z spectrum (inset). The peaks corresponding to the intact compound, carrying the indicated number of charges (protons), are evidenced.

Table S1: Analytical parameters of Fe^{III}- MC-6 analogs.

Fe^{III}-MC6 analogs	**t_R (min)**	**Measured mass (Da)**	**Theoretical mass (Da)**
$E^2L(TD)$	49.49	3535.42±0.08	3536.75
$R^{10}L(TD)$	48.51	3508.90±1.60	3509.67
$E^2L(D)$	50.09	3536.06±0.92	3536.75
$R^{10}L(D)$	48.81	3507.06±0.66	3509.67

Kinetic characterization of peroxidase-like catalytic activity of MC-6 analogs

The initial rates of ABTS oxidation (v_0) are plotted as a function of both substrates concentration. Data were fitted according to two-substrate Michaelis–Menten kinetics (eq.1, main text).

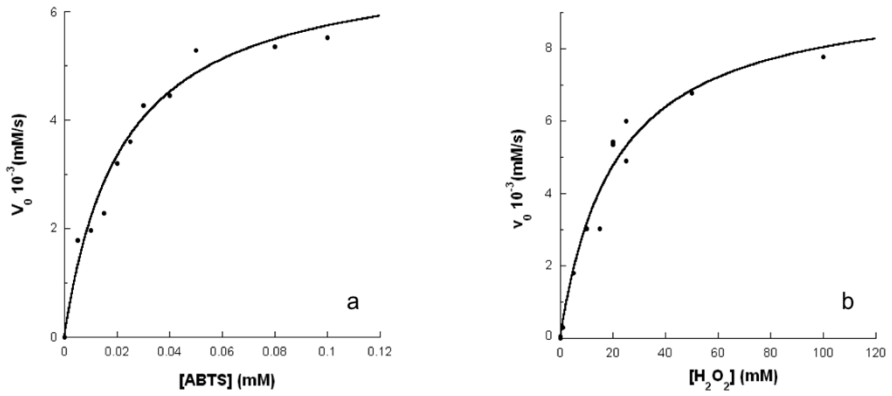

Figure S6: Peroxidase-like activity of Fe^{III}–E^2L(*TD*)-MC-6. a). Dependence towards ABTS: reaction conditions were E^2L(*TD*)-MC-6 (20 nM), H_2O_2 (20 mM) in 50 mM phosphate buffer pH 6.5/TFE (1:1 v/v). b). Dependence towards H_2O_2: reaction conditions were E^2L(*TD*)-MC-6 (20 nM), ABTS (0.10 mM) in 50 mM phosphate buffer pH 6.5/TFE (1:1 v/v).

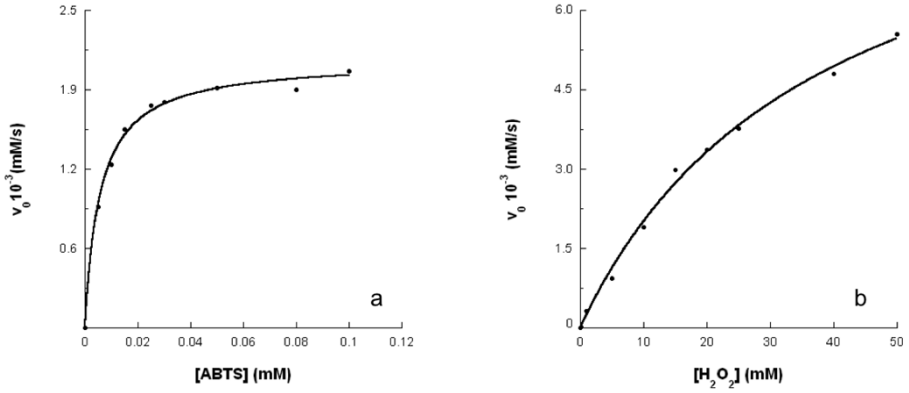

Figure S7: Peroxidase-like activity of Fe^{III}–R^{10}L(*TD*)-MC-6. a). Dependence towards ABTS: reaction conditions were R^{10}L(*TD*)-MC-6 (20 nM), H_2O_2 (10 mM) in 50 mM phosphate buffer pH 6.5/TFE (1:1 v/v). b). Dependence towards H_2O_2: reaction conditions were R^{10}L(*TD*)-MC-6 (20 nM), ABTS (0.10 mM) in 50 mM phosphate buffer pH 6.5/TFE (1:1 v/v).

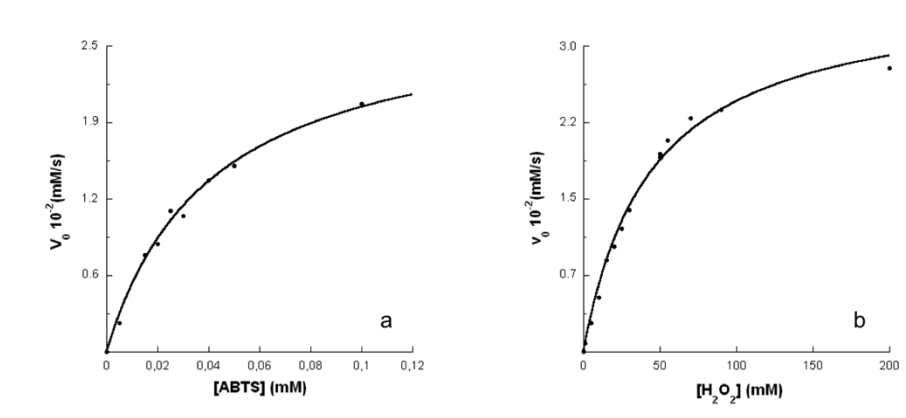

Figure S8: Peroxidase-like activity of Fe^{III}–E^2L(*D*)-MC-6. a). Dependence towards ABTS: reaction conditions were E^2L(*D*)-MC-6 (0.20 μM), H_2O_2 (50 mM) in 50 mM phosphate buffer pH 6.5/TFE (1:1 v/v). b). Dependence towards H_2O_2: reaction conditions were E^2L(*D*)-MC-6 (0.20 μM), ABTS (0.10 mM) in 50 mM phosphate buffer pH 6.5/TFE (1:1 v/v).

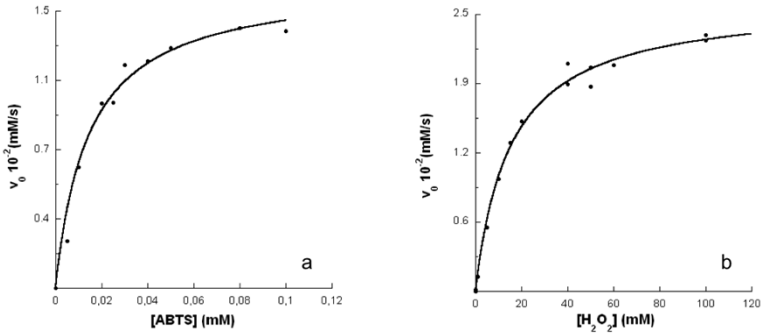

Figure S9: Peroxidase-like activity of Fe^{III}–R^{10}L(*D*)-MC-6. a). Dependence towards ABTS: reaction conditions were R^{10}L D MC-6 (0.20 μM), H_2O_2 (20 mM) in 50 mM phosphate buffer pH 6.5/TFE (1:1 v/v). b). Dependence towards H_2O_2: reaction conditions were R^{10}L D MC-6 (0.20 μM), ABTS (0.10 mM) in 50 mM phosphate buffer pH 6.5/TFE (1:1 v/v) .

Oxidation mechanism of E²L(*TD*)-MC6: the formation of a compound I analog

UV-vis spectroscopy was used to investigate the reaction of ferric E²L(*TD*)-MC6 and hydrogen peroxide in the absence of co-substrates. Upon addition of 1 equivalent of H_2O_2, the Soret band intensity decreased of more than 50% (no λ shifts), and α/β bands flattened, indicating the formation of porphyrin radical intermediates (Fig.3).[2] These spectral changes, observed within one minute, describe a peroxidase-analogue compound I, which was stable for 15 minutes. Thus, the spontaneous decay to the ferric state occurred almost reversibly. The whole cycle $Fe^{III} \rightarrow Fe^{IV}=O^{*+} \rightarrow Fe^{III}$ was completed in about 2 hours.

In the examined experimental conditions, there were no evidences of compound II formation, suggesting that the reaction may proceed through a single two-electron transfer, instead of two consecutive one-electron pathways.[1] Rapid-scan stopped flow analyses are in progress to elucidate the catalytic mechanism and the rate-limiting steps of the reaction.

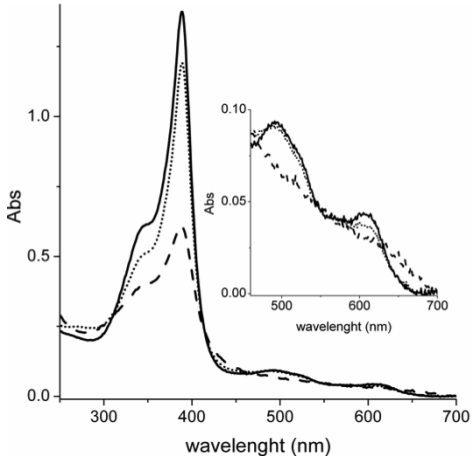

Figure S 10: Reaction of Fe^{III}-E²L(*TD*)-MC6 with H_2O_2. UV-vis spectra of Fe^{III}-resting state (solid line), of $Fe^{IV}=O^{*+}$ compound I (dashed line) obtained by addition of 1 equivalent of H_2O_2, and of Fe^{III}-resting state (dotted line), regenerated after spontaneous decay of compound I. Inset: visible region. Reaction conditions were: $2.0 \cdot 10^{-5}$ M E²L(*TD*)-MC6, in 50 mM phosphate buffer pH 6.5/TFE (1:1 v/v), T=25°C.

The absorbance changes were monitored upon H_2O_2 addition and spectra were recorded in 250-700 wavelength range, with a 9600 nm/min scan rate, 2.0 nm data interval and an average time of 0.0125 s. Temperature was set at 25°C and the reaction mixture was magnetically stirred.

Spectroscopic characterization of ferric complex of E²L(*TD*)-MC-6 analog

Table S2: Electronic absorption spectral features of Fe^{III}-E^2L(*TD*)-MC6, at different pH values.

		UV-vis Absorption			
pH	**TFE**	**Soret/nm (ε 10^{-4}/ M^{-1} cm^{-1})**	**Vis/nm (ε 10^{-3}/ M^{-1} cm^{-1})**		
2.0	50%	386 nm (10)	495 nm (5.0)	529 nm (0.40)	618 nm (0.23)
4.7	50%	387 nm (9.0)	493 nm (4.9)		617 nm (0.20)
6.5	50%	388 nm (7.6)	493 nm (4.9)		608 nm (0.25)
9.0	50%	389 nm (6.3) 341 nm (4.3)	488 nm (5.5)	518 nm (0.50)	604 nm (0.36)

Table S3: MCD spectral features of Fe^{III}-E^2L(*TD*)-MC6, at different pH values.

		MCD	
pH	**TFE**	**Soret/nm ($\Delta\varepsilon_M$/M^{-1} cm^{-1} T^{-1})**	**Vis/nm ($\Delta\varepsilon_M$/M^{-1} cm^{-1} T^{-1})**
2.0	50%	366 nm (sh, 4.2) 382 nm (11.0) 388 nm (0) 394 nm (-12.0)	477 nm (1.9) 503 nm (0) 521 nm (1.1) 528 nm (0) 540 nm (-2.7) 597 nm (0.1) 591 nm (1.2) 629 nm (-1.3)
4.7	50%	365 nm (sh, 2.9) 383 nm (11.2) 390 nm (0) 394 nm (-10.3)	475 nm (1.2) 499 nm (0) 518 nm (0.1) 538 nm (-1.9) 598 nm (0.1) 629 nm (-1.8)
6.5	50%	385 nm (11.5) 393 nm (0) 402 nm (-8.9)	471 nm (1.5) 509 nm (0.7) 538 nm (-1.9) 574 nm (0) 593 nm (0.7) 627 nm (-1.9)
9.0	50%	388 nm (12.5) 396 nm (0) 404 nm (-9.8)	467 nm (1.0) 511 nm (0.6) 533 nm (-2.5) 566 nm (0) 593 nm (1.2) 602 nm (0) 620 nm (-2.1)

Table S4: Far-UV region CD spectral features of Fe^{III}-E^2L(*TD*)-MC6, at different pH values and TFE concentrations.

		Far-UV CD			
pH	**TFE**	**λ_{min}/nm (-θ_{min} 10^{-4}/ deg cm^{2}dmol^{-1}res^{-1})**	**-θ_{222} 10^{-4}/ deg cm^{2}dmol^{-1}res^{-1}**	**θ_{ratio}**	**λ_0**
4.7	50%	207 nm (1.5)	1.15	0.77	199
6.5	50%	207 nm (1.4)	1.09	0.78	199
4.7	0%	202 nm (0.97)	0.31	0.32	192
4.7	10%	205 nm (1.0)	0.52	0.52	197
4.7	25%	207 nm (1.4)	1.06	0.76	199
4.7	50%	207 nm (1.5)	1.15	0.77	199

Table S5: Soret region CD spectral features of Fe^{III}-E^2L(*TD*)-MC6, at different pH values and TFE concentrations.

		Soret CD	
pH	**TFE**	**λ_{min}/nm**	**-θ_{386} 10^{-4}/ deg cm^2 dmol^{-1})**
4.7	50%	386	1.5
6.5	50%	386	0.9
4.7	0%	386	~ 0
4.7	10%	386	0.3
4.7	25%	386	0.8
4.7	50%	386	1.5

Model equation for pH-dependent equilibria of Fe^{III}-$E^2L(TD)$-MC6 analog

The pH-dependent equilibrium is described by the following equation:

$$AH^{2+}_2 \overset{K_{a1}}{\leftrightarrow} AH^+ + H^+ \overset{K_{a2}}{\leftrightarrow} A^- + H^+ \quad (Eq.\,1)$$

The equilibrium constants, K_{a1} and K_{a2}, can be expressed as:

$$K_{a1} = \frac{[AH^+] \cdot [H^+]}{[AH^{2+}_2]} \qquad ; \qquad K_{a2} = \frac{[A^-] \cdot [H^+]}{[AH^+]} \quad (Eq.\,2)$$

The total concentration (C_{tot}) of the MC6 analogue can be expressed as sum of the three species:

$$C_{tot} = [A^-] + [AH^+] + [AH^{2+}_2] \quad (Eq.3)$$

The total absorbance and the total concentration can be expressed as he sum of the contribution of all the three species, which can be indicated in dependence of $[A^-]$:

$$Abs_{tot} = \varepsilon_3 \cdot [A^-] + \varepsilon_2 \cdot \frac{[A^-] \cdot [H^+]}{K_{a2}} + \varepsilon_1 \cdot \frac{[A^-] \cdot [H^+]^2}{K_{a1} \cdot K_{a2}} \quad (Eq.4)$$

$$C_{tot} = [A^-] + \frac{[A^-] \cdot [H^+]}{K_{a2}} + \frac{[A^-] \cdot [H^+]^2}{K_{a1} \cdot K_{a2}} \quad (Eq.5)$$

Equations 4 and 5 can be rearranged, giving:

$$Abs_{tot} = \frac{C_{tot} \cdot \left(\varepsilon_3 + \varepsilon_2 \cdot \frac{[H^+]}{K_{a2}} + \varepsilon_1 \cdot \frac{[H^+]^2}{K_{a1} \cdot K_{a2}}\right)}{\left(1 + \frac{[H^+]}{K_{a2}} + \frac{[H^+]^2}{K_{a1} \cdot K_{a2}}\right)} \quad (Eq.6)$$

Equation 6 can be written as:

$$Abs_{tot} = \frac{\left(Abs_3 + Abs_2 \cdot \frac{[H^+]}{K_{a2}} + Abs_1 \cdot \frac{[H^+]^2}{K_{a1} \cdot K_{a2}}\right)}{\left(1 + \frac{[H^+]}{K_{a2}} + \frac{[H^+]^2}{K_{a1} \cdot K_{a2}}\right)} \quad (Eq.7)$$

Abs_i parameters represent the absorbance of the three differently protonated species. Equation 7 was used to fit the observed Abs Soret data plot (fig. 1, main text), which was then reported as ε_{387}, considering Fe^{III}-E^2L(*TD*)-MC-6 molar concentration (7.0 μM) and the cell path length (1.0 cm).

*** References***

1. F. Nastri, L. Lista, P. Ringhieri, R. Vitale, M. Faiella, C. Andreozzi, P. Travascio, O. Maglio, A. Lombardi, and V. Pavone, *Chem. - Eur. J.*, 2011, **17**, 4444–4453.

2. M. Faiella, O. Maglio, F. Nastri, A. Lombardi, L. Lista, W. R. Hagen, and V. Pavone, *Chem. - Eur. J.*, 2012, **18**, 15960–15971.

3. P. Sieber, *Tetrahedron Lett.*, 1987, **28**, 2107–2110.

4. Buchler, J.W.,, in *The Porphyrins*, NY, USA, Academic Press., 1979, vol. I, pp. 389–483.

5. F. Nastri, A. Lombardi, G. Morelli, O. Maglio, G. D'Auria, C. Pedone, and V. Pavone, *Chem. - Eur. J.*, 1997, **3**, 340–349.